Clays and Clay Minerals, Vol. 50, No. 1, 99–110, 2002.

MICROBIOTIC FORMATION OF SILICATE MINERALS IN THE WEATHERING ENVIRONMENT OF A PYROCLASTIC DEPOSIT

MOTOHARU KAWANO[1,*] AND KATSUTOSHI TOMITA[2]

[1] Department of Biochemical Sciences and Technology, Faculty of Agriculture, Kagoshima University, 1-21-24 Korimoto, Kagoshima 890-0065, Japan

[2] Department of Earth and Environmental Sciences, Faculty of Science, Kagoshima University, 1-21-35 Korimoto, Kagoshima 890-0065, Japan

Abstract—Bacterial mineralization in weathered pyroclastic deposits of the Kaimondake volcanic ash (4040 ybp) and the Koya pyroclastic flow (6400 ybp) was investigated to evaluate the impacts of bacteria on mineral formation, and to characterize the microbiogenic minerals in the weathering environment. The mineralogy of abiogenic weathering products was also investigated for comparison with the microbiogenic products, and mineral saturation indices were calculated for porewaters using the PHREEQC computer code. The results indicated that these weathered pyroclastic deposits contain 10^8–10^9 cells/g, consisting of spherical to rod-shaped bacteria. Associated abiogenic allophane had an Al/Si ratio ranging from 1.01 to 2.13. The bacterial cell surfaces were completely or partially covered by poorly-ordered silicate minerals, which could be divided into two groups based on their chemical and morphological characteristics. Group I was characterized by well developed fibrous to smectite-like flaky habits with variable Al, Si and Fe, corresponding to compositions between proto-imogolite allophane and chamosite. These Al-Si-Fe minerals were the most abundant and major microbiogenic products in both lithologies. Group II exhibited poorly-developed aggregates of allophane-like granular materials composed mainly of Al and Si with minor Fe. Geochemical calculations revealed that the porewaters were saturated with respect to allophane and other crystalline clay minerals such as halloysite, kaolinite, montmorillonite and nontronite. These microbiogenic minerals may be formed as the earliest phase of these clay minerals after interaction of the bacterial cell surfaces with dissolved cations mainly Si, Al and Fe, in the porewaters.

Key Words—Allophane, Bacteria, Bacterial Mineralization, Cell Surface, Pyroclastic Deposit, Silicate Mineral, Weathering.

INTRODUCTION

Bacteria accumulate solute ions and precipitate minerals on their cell surfaces. This process is initiated by the binding of metal ions to negatively charged substances such as carboxyl or phosphoryl groups in the structural polymers of cell walls, followed by nucleation and mineral growth (Beveridge, 1989; Schultze-Lam *et al*., 1996; Fein *et al*., 1997). Such bacterial mineralization is a common and widespread phenomenon occurring in various geochemical environments where liquid water is available. For example, bacterial mineralization in hot springs has been observed to form amorphous silica (Schultze-Lam *et al*., 1995; Hinman and Lindstrom, 1996; Jones and Renaut, 1996), Fe-silica minerals in successive stages of crystallization (Ferris *et al*., 1986; Tazaki, 2000), and calcite (Tazaki *et al*., 1995; Fouke *et al*., 2000). Another well known example is the formation of Fe oxide or Fe sulfate minerals in acid mine drainage (Ferris *et al*., 1989; Bigham *et al*., 1990; Fortin and Beveridge, 1997), acid sulfate soils (Fitzpatrick *et al*., 1992), and in seafloor hydrothermal vents (Hannington and Jonasson, 1992; Fortin *et al*., 1998). Bacteria also interact with dissolved ions and precipitate poorly-ordered silicate minerals with a chamositic composition in river and lake sediments (Ferris *et al*., 1987; Konhauser, 1998; Konhauser *et al*., 1998). Recent geobiological studies indicate that such mineralization has occurred from as early as 3.5 billion years ago (*e.g*. Schopf, 1983), and the total mass of microbiogenic minerals has been estimated to approach that of the Earth's total exposed land mass (Beveridge and Fyfe, 1985).

There is little information about impacts of bacteria on geochemical cycles in the terrestrial weathering environments of rocks and sediments, These environments are distributed over the Earth's surface, and are a major habitat of bacteria, with populations ranging from 10^6 to 10^9 cells/g, much higher than the putative 10^5 cells/ml of freshwater and marine environments (Ehrlich, 1990; Barns and Nierzwicki-Bauer, 1997). The abundance of these bacteria dictates that they will have a significant effect on geochemical processes, and on the flux of chemical compounds linked to global environmental issues (Ehrlich, 1990). In this study, we investigated the impact of bacteria on the formation of secondary minerals in the weathering environments of pyroclastic deposits distributed around southern parts of Kagoshima Prefecture, Japan. The results reveal that there are great amounts of bacteria in the deposits, and

* E-mail address of corresponding author:
kawano@chem.agri.kag oshima-u.ac.jp

that they have significant impacts on the formation of secondary silicate minerals during weathering processes. The mineralogical characteristics of these microbiogenic products, and their possible formation processes, are presented in this paper.

MATERIALS

Weathered pyroclastic deposits distributed in the southern parts of Satsuma Peninsula, Kagoshima Prefecture, Japan, were examined in this study (Figure 1). This area is underlain by Pliocene to Pleistocene andesitic rocks. Above these are the Koya rhyolitic pyroclastic flow (K2) and the Kaimondake basaltic volcanic ash (K1). The K1 deposit is distributed in the southern parts of both Satsuma and Osumi Peninsula. This pyroclastic material was ejected ~4040 y ago from Mt. Kaimondake, ~12 km southwest of the sampling point (Ishikawa *et al.*, 1979). The K2 deposit is distributed over much of eastern to central Japan including all of Kagoshima Prefecture. This material was ejected ~6400 y ago from Kikai caldera, ~70 km south of the sampling point (Ui and Fukuyama, 1972).

Samples were collected from a newly exposed road cut in which flat-lying exposures of K1 (60–70 cm thick) and the underlying K2 (100–110 cm thick) were clearly observed. The surface of the uppermost K1 deposit was covered by vegetation and the deposit was black due to included organic substances. The K2 deposit was brown to orange in color due to Fe oxidation during weathering. Two samples were collected: from the K1 deposit ~30 cm below the ground surface, and from the K2 deposit at a depth of ~90 cm (Figure 1). These samples were immediately sealed in a plastic bag to avoid biological contamination and water loss by evaporation.

EXPERIMENTAL METHODS

Mineralogy of pyroclastics

X-ray diffraction (XRD) analysis was conducted using a RIGAKU RU-200 diffractometer (CuKα radiation, 30 kV, 100 mA) equipped with a graphite monochromater. Bulk samples were powdered and loaded into glass holders. Clay fractions (<2 μm) were collected by sedimentation in distilled water and centrifuged, then deposited as oriented mounts onto glass slides. Quantitative estimates of the constituents were obtained by an internal standard XRD method (Kawano and Tomita, 1999).

Scanning electron microscopy (SEM) of carbon-coated samples was performed with an HITACHI S-4100 scanning electron microscope equipped with a

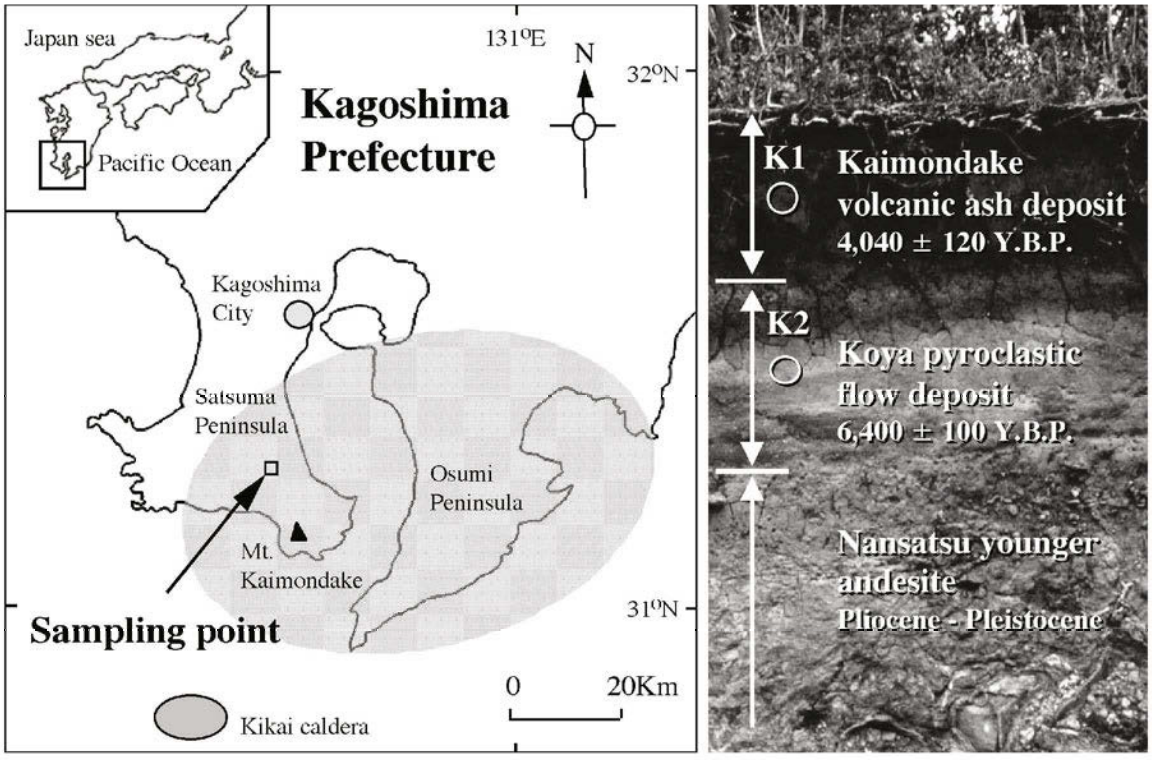

Figure 1. Map of Kagoshima Prefecture, southern Kyushu, Japan, showing the location of the sampling point of weathered pyroclastics used in this study, and a photograph of the pyroclastic deposits. The samples were collected from the Kaimondake volcanic ash (K1) deposit at a depth of ~30 cm below the ground surface, and from the Koya pyroclastic flow (K2) deposit at a depth of ~90 cm. The shaded area on the map signifies the area over which Kaimondake volcanic ash was spread.

https://doi.org/10.1346/000986002761002865 Published online by Cambridge University Press

LINK ISIS energy dispersive spectrometry (EDS) system, operated at an accelerating voltage of 15 kV. The EDS spectra were obtained using electron-beam spot sizes of ~1–2 μm, and a live time of 60 s. Bulk samples were fused with $Li_2B_4O_7$ prior to analysis. The chemical analyses of volcanic glass, plagioclase, olivine and pyroxene were performed using hand-picked grains mounted on carbon stubs. The quantification was carried out using a standard of basaltic glass with composition of 53.03% SiO_2, 1.32% TiO_2, 14.75% Al_2O_3, 9.25% Fe_2O_3, 0.15% MnO, 7.88% MgO, 9.38% CaO, 2.79% Na_2O and 1.44% K_2O; FeS_2 was also used as a standard for S. The accuracy of the quantification was ±1–5 wt.% for each element.

Ion-exchange experiments were conducted using 10.0 mM NaCl solution to remove adsorbed ions on the surfaces of weathering products. Solutions for experimentation were made by adjusting the pH of the NaCl stock solution to make individual solutions of pH 3.0 to 10.0 in steps of pH 1.0, by the addition of HCl or NaOH. About 10 mg of each clay fraction was mixed with 50 ml of each NaCl solution, and this mixture was shaken for 1 h and then centrifuged. After washing with 80% ethanol until Cl^--free, the clay fractions were dried on carbon stubs and used for EDS analysis.

The Fe precipitates on the surface of weathering products were dissolved selectively using dithionite citrate bicarbonate extraction (Mehra and Jackson, 1960).

Solution chemistry

Moisture contents were measured by drying ~10 g of moist samples at 25°C for 5 d. Porewaters were collected using an hydraulic press. About 200 g of each sample were pressed slowly to a confining pressure of 500 kg/cm^2, yielding ~20–30 ml of porewater. The porewaters were centrifuged and filtered using 0.2 μm Minisart membranes prior to chemical analysis. The chemical analysis was by colorimetric analysis for total dissolved Si, by atomic adsorption spectroscopy for total Fe, Al, Mn, Mg, Ca, Na and K, and by ion chromatography for F, Cl, NO_3, PO_4 and SO_4. Fe(II) was determined by colorimetric analysis using the phenanthroline colorimetric method. The Fe(III) was obtained by difference between Fe(II) and total Fe. The pH and Eh values were measured using a glass electrode. Temperature was measured in the field.

Geochemical calculations were performed using the PHREEQC Ver. 2 geochemical code (Parkhurst and Appelo, 1999) using the MINTEQ.DAT thermodynamic database supplied with PHREEQC. We added the solubility data of allophane (Percival, 1995) to MINTEQ.DAT. The solution chemistry data were input to PHREEQC without modification, except that trace ions (F and PO_4) below the detection limit were ignored. We used the field water temperature of 23.5°C, and a CO_2(g) partial pressure of $10^{-3.5}$.

Bacterial mineralization

Bacterial mineralization was examined by transmission electron microscopy (TEM) using a JEOL 2000 FX microscope with LINK ISIS EDS operated at an accelerating voltage of 200 KeV using a carbon-coated sample on a Cu grid. The EDS was collected using an electron-beam spot size <50 nm over 100 s live time. Quantification was by a thin-film K-factor method (Jiang *et al*, 1994), using the basaltic glass described above for Si, Al, Fe and Ti. Each moist sample was mixed 1:1000 (dry weight basis) with sterilized-distilled water and homogenized ultrasonically (60 Hz, 40 W) and shaken for a few minutes, then 0.005 ml of the suspension was dropped onto a Cu grid using a micro pipette. The Cu grid was 3.0 mm in diameter with 150 circular holes 0.117 mm in diameter, and the area ratio of a hole to the whole grid was $\sim 1.52 \times 10^{-3}$. The number of bacteria observed in the grid holes was counted directly and the total number in 1.0 g of sample was calculated as follows:

$$N = n/(5 \times 1.52 \times 10^{-9}),$$

where N was the total number of bacteria in 1.0 g of sample and n was the number of bacteria observed in each grid hole. Selected area electron diffraction (SAED) was performed on the microbiogenic minerals using a focal length of 1347 mm.

RESULTS

Mineralogy and chemistry of pyroclastic material

The K1 deposit consisted of 50–60 wt.% volcanic glass, 10–20 wt.% plagioclase ($Ab_{31}An_{68}$), <10 wt.% olivine ($Fo_{51}Fa_{49}$) and augite, and very minor magnetite. The K2 deposit consisted of 50–60 wt.% volcanic glass exhibiting fine to blocky size fragments, <20 wt.% plagioclase ($Ab_{53}An_{47}$), and trace amounts of augite. The chemical compositions of bulk samples and volcanic glasses are listed in Table 1. Both K1 and K2 deposits also contained variable amounts of poorly-ordered weathering products composed mainly of allophane. The clay-sized fraction of K1 showed broad diffraction peaks at about 4.4, 3.3, 2.6 and 2.3 Å, all characteristic of Si-rich allophane, *i.e.* 'proto-halloysite allophane' (Wada *et al*., 1988). On the other hand K2 exhibited two broad peaks at ~3.4 and 2.3 Å, compatible with reflections of Al-rich allophane, *i.e.* 'proto-imogolite allophane' (Farmer *et al*., 1979). The TEM confirmed the presence of 30–40 nm allophane spheres and trace amounts of imogolite tubes with a width of ~20 nm. The allophane in K1 had higher Si and lower Al relative to K2, and both allophanes were apparently enriched in Fe (Table 1).

Solution chemistry

The moisture contents of K1 and K2 were 52 and 53 wt.%, respectively. The porewaters were slightly

https://doi.org/10.1346/000986002761002865 Published online by Cambridge University Press

Table 1. Chemical compositions of bulk samples, volcanic glass, and allophane.

	K1			K2		
	Bulk	Glass	Allophane	Bulk	Glass	Allophane
SiO_2	45.11	71.4	39.28	46.49	74.99	34.32
TiO_2	1.89	1.58	1.23	1.86	0.91	1.37
Al_2O_3	25.02	9.20	44.89	29.74	8.76	51.21
Fe_2O_3	24.23	6.80	12.23	15.76	5.92	9.16
MnO	0.28	–	–	0.07	–	–
MgO	0.09	0.02	–	0.15	0.05	–
CaO	1.60	3.15	–	3.27	2.94	–
Na_2O	0.15	3.19	–	1.43	2.06	–
K_2O	1.63	4.67	0.70	1.23	4.37	0.13
SO_3	–	–	1.66	–	–	3.82
Total (%)	100.00	100.00	100.00	100.00	100.00	100.00

Total Fe as Fe_2O_3. The wt.% of oxide compounds were normalized to 100% total. The chemical analyses of allophane are average values of 20 aggregates, respectively. K1 and K2 represent the Kaimondake volcanic ash and Koya pyroclastic flow deposits, respectively.

acidic, had low redox potential, and contained significant Si, Al and total Fe (Table 2). Figure 2a shows the activities of H_4SiO_4, Al^{3+} and Fe^{3+} ions plotted on a phase diagram of corresponding predicted oxide and hydroxide minerals at 23.5°C, calculated by PHREEQC. The porewater of K1 was slightly undersaturated with respect to amorphous silica and amorphous $Al(OH)_3$, but supersaturated with respect to gibbsite, ferrihydrite and hematite. The porewater of K2 was reasonably saturated with respect to amorphous silica and amorphous $Al(OH)_3$, and was also supersaturated with respect to gibbsite, ferrihydrite and hematite. The porewaters were apparently supersaturated with respect to allophane, halloysite and kaolinite (Figure 2b). In addition, the geochemical calculations confirmed that the porewaters were greatly supersaturated with respect to montmorillonite and nontronite (Table 3).

Table 2. Temperature and solution chemistry of the porewaters.

	K1	K2
Temp (°C)	23.5	23.5
pH	4.97	5.71
Eh (mV)	114	68
Si	27.21 mg/L	54.57 mg/L
Al	0.49	0.24
Fe(III)	0.54	7.07
Fe(II)	0.35	2.67
Mn	0.033	0.059
Mg	1.576	0.157
Ca	1.483	0.087
Na	9.72	10.16
K	1.52	2.19
F^-	<0.01	<0.01
Cl^-	10.41	2.45
NO_3^-	8.57	0.01
PO_4^{3-}	<0.01	<0.01
SO_4^{2-}	3.35	0.92

Secondary minerals formed by abiotic processes

As determined by XRD, allophane was the most abundant secondary mineral in K1 and K2. In both samples, allophane occurred as blocky or spherical aggregates with a size of <1.0 μm (Figure 3). The chemical compositions of allophanes plotted on a ternary diagram of Al-Si-Fe system (Figure 4) indicate some variability in composition with Al/Si ratios ranging from 1.01 to 1.67 for K1 and 1.33 to 2.13 for K2. The average Al/Si ratio of allophanes in K2 (Al/Si = 1.76) was significantly greater than that of K1 (Al/Si = 1.37). This is in good agreement with their XRD profiles (not shown), in which K1 and K2 showed Si-rich and Al-rich characteristics, respectively. The allophanes also contained variable amounts of Fe with Fe/Si ratios ranging from 0.14 to 0.48 for K1 and 0.09 to 0.39 for K2. The average Fe/Si ratios of K1 and K2 are 0.24 and 0.20, respectively. These Fe ions were readily removed and the Fe/Si ratios decreased to <0.03 after DCB extraction. This result suggests that Fe was precipitated on the allophane surfaces as very fine non-crystalline Fe hydroxide and was not substituted for Al in the allophane structure. Additionally, the allophane con-

Table 3. Solubility products (log *K*) and saturation indices (*SI*) of predicted minerals at 23.5°C.

Mineral	log *K* (23.5°C)	*SI* (K1)	*SI* (K2)
Amorphous silica	−2.72	−0.30	0.01
Amorphous $Al(OH)_3$	10.48	−0.81	−0.02
Gibbsite	8.85	0.81	1.60
Ferrihydrite	4.89	0.71	2.58
Hematite	−3.89	15.09	18.83
Allophane	24.16	8.45	12.25
Halloysite	9.14	4.13	6.35
Kaolinite	5.86	7.42	9.63
Montmorillonite	2.67	6.31	9.52
Na-nontronite	−14.50	18.30	23.71

https://doi.org/10.1346/000986002761002865 Published online by Cambridge University Press

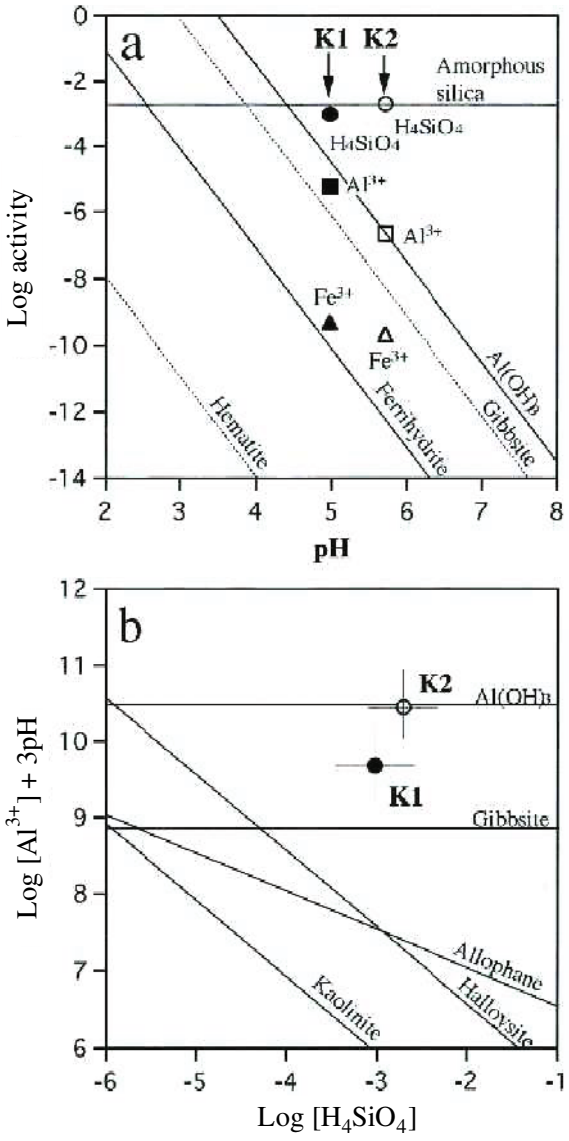

Figure 2. Solution chemistry of porewaters in the Kaimondake volcanic ash (K1) and the Koya pyroclastic flow (K2) deposits plotted on the phase diagram of amorphous silica, amorphous $Al(OH)_3$, gibbsite, ferrihydrite and hematite (a), and on that of allophane, halloysite and kaolinite (b) at a temperature of 23.5°C.

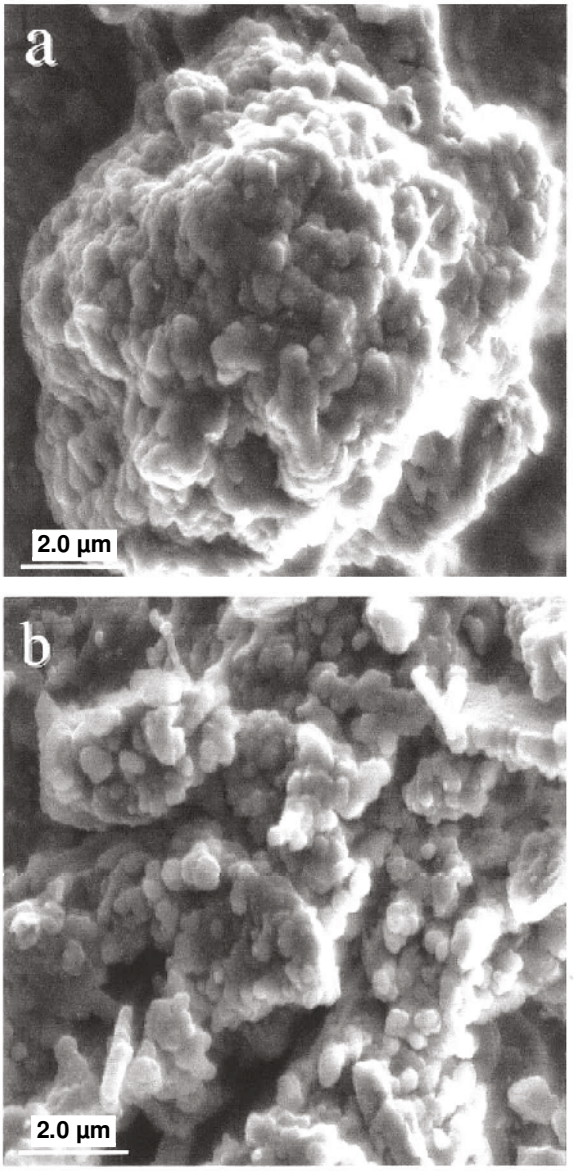

Figure 3. SEM micrographs of allophanes formed by abiotic weathering processes in the Kaimondake volcanic ash (a) and the Koya pyroclastic flow (b) deposits.

tained minor and variable amounts of Ti, K and S. It is noteworthy that the Ti/Si ratios were positively correlated with Fe/Si, but not with Al/Si. Thus, Ti ions might be precipitated with the non-crystalline Fe hydroxide on the allophane surfaces. The K and S ions were completely exchanged by Na and Cl by ion exchange experiments, suggesting that the K and S were adsorbed on allophane surfaces.

Number of bacteria

The TEM observations showed abundant deposits of 1.0 to 2.0 µm spherical to rod-shaped bacteria on K1 and K2. About 20 to 30 cells were observed in each grid hole for K1, and ~5–10 cells/hole for K2. The number of bacteria in K1 was thus 2.6×10^9 to 3.9×10^9 cells/g, and in K2 was 6.6 x 10^8 to 1.3 x 10^9 cells/g. These populations were close to the bacterial numbers in soil environments (Barns and Nierzwicki-Bauer, 1997).

Secondary minerals formed on the bacterial surfaces

Most bacteria in K1 were covered by thin fibrous minerals <0.2 µm wide (Figure 5a). The electron diffraction pattern showed a diffuse halo with no conspicuous spots or rings, suggesting a poorly-ordered structure. The EDS revealed that these poorly-ordered

https://doi.org/10.1346/000986002761002865 Published online by Cambridge University Press

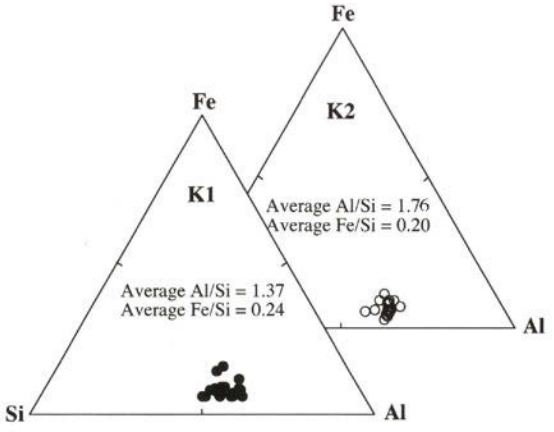

Figure 4. Chemical compositions of allophanes in the Kaimondake volcanic ash (closed circles) and the Koya pyroclastic flow (open circles) deposits plotted on the ternary diagrams of the Al-Si-Fe system.

Table 4. Chemical characteristics of allophane and microbiogenic minerals in the weathered pyroclastic deposits.

	K1	K2
Abiogenic allophane (20)		
Average Al/Si ratio	1.37	1.76
Average Fe/Si ratio	0.24	0.20
Average Ti/Si ratio	0.03	0.03
Microbiogenic Group I (6)		
Average Al/Si ratio	2.02	1.94
Average Fe/Si ratio	1.28	1.18
Average Ti/Si ratio	0.23	0.23
Microbiogenic Group II (4)		
Average Al/Si ratio	2.14	1.87
Average Fe/Si ratio	0.05	0.03
Average Ti/Si ratio	0.02	0.00

Microbiogenic Group I and II represent Al-Si-Fe and Al-Si minerals associated with bacteria, respectively. The numbers in parentheses signify the number of samples used for calculation of average atomic ratios.

materials were predominantly Al, Si and Fe, with small amounts of Ti, S and Cl (Figure 5b). These Al-Si-Fe minerals were the most abundant products associated with bacteria in this deposit. In addition, the K1 deposit contained some fragments of fungoid hyphae exhibiting a tubular habit (0.5–1.0 μm wide), which were usually coated by aggregates of fine granular allophane-like particles with a thickness of <0.2 μm (Figure 5c). These precipitates were characteristically enriched in Al and Si, and very depleted in Fe and Ti (Figure 5d). Electron diffraction of these particles also showed diffuse haloes, indicating a poorly-ordered structure. In K2, similar spherical and rod-shaped or ellipsoidal bacteria with sizes of 1.0–2.0 μm were common, also usually covered by well developed precipitates of poorly-ordered Al-Si-Fe minerals. Figure 6a shows a typical example of a spherical bacterium with a cell size of ~1.5 μm, on which are aggregates of smectite-like flaky minerals up to 0.5 μm thick. The flaky minerals consisted of Al, Si and Fe, with small amounts of Ti and Mn (Figure 6b). Some spherical bacteria with extracellular massive or curdy precipitates of granular material were observed, composed of Al and Si, with minor Fe and Ti (Figure 6c,d).

These secondary minerals produced on the bacterial surfaces can be divided into two groups based on their chemical and morphological characteristics. Group I corresponds to the poorly-ordered fibrous to flaky minerals enriched in Al, Si and Fe (Figures 6a and 7a). Group II can be characterized by the massive or curdy aggregates of fine granular particles consisting mainly of Al and Si, with little Fe (Figures 6c, 7c). A ternary plot of Al, Si and Fe, with the ideal compositions of some related clay minerals, is presented in Figure 7. In this diagram, it appears that Group I has a wide range of chemical compositions between proto-imogolite allophane (Fe/Si = 0) and chamosite (Fe/Si = 1.7), while Group II is consistent with a composition of proto-imogolite allophane. The chemical compositions of both groups are also significantly different from those of allophane plotted on the same diagram in Figure 5. The average Al/Si, Fe/Si and Ti/Si ratios of the allophane and two groups of microbiogenic minerals are summarized in Table 4. Group I is enriched in Al, Fe and Ti relative to abiogenic allophane, whereas the Group II is enriched in Al and depleted in Fe and Ti. These chemical characteristics suggest that the two groups of microbiogenic minerals were produced by processes other than those responsible for abiotic allophane, and they may be at different stages of mineralogy than reference allophane.

Another example of a rod-shaped bacterium with poorly-ordered extracellular Al-Si-Fe minerals belonging to Group II is given in Figure 8. This micrograph clearly shows partial degradation of the bacterial cell, and dispersion of the Al-Si-Fe minerals surrounding the cell surface into the extracellular environment. Similar cells exhibiting partially degraded or decomposed forms are occasionally observed together with fragments or aggregates of fibrous minerals detached from the cell surfaces.

DISCUSSION

Weathering conditions

Generally, the formation of secondary minerals in weathering environments proceeds by initial precipitation of a non-crystalline or poorly-ordered metastable phase, followed by subsequent recrystallization to a more stable phase. In the present weathering environment, the pyroclastic deposits include porewaters make up ~52–53 wt.%, and which are slightly acidic and have relatively low redox potential. The geochemical calculations indicate that the porewaters are saturated with respect to gibbsite, ferrihydrite and hematite when only

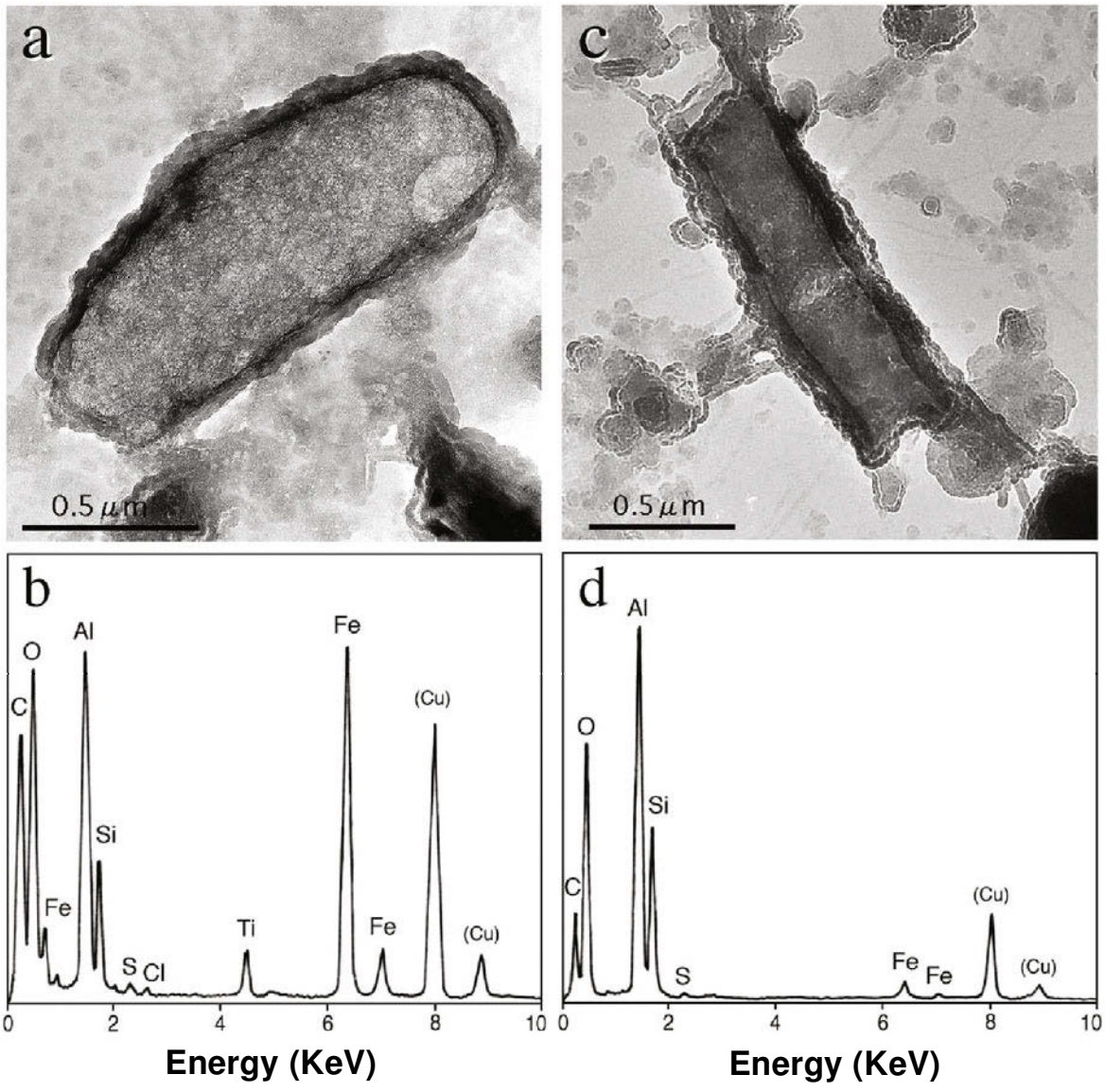

Figure 5. TEM micrographs and EDX spectra of: (a,b) microbiogenic poorly-ordered Al-Si-Fe minerals formed on the cell surface of a rod-shaped bacterium; (c,d) granular precipitates of poorly-ordered Al-Si minerals associated with a fragment of a fungoid hypha in the Kaimondake volcanic ash deposit.

Fe is considered; with respect to allophane, halloysite and kaolinite when Al and Si are considered; and with respect to montmorillonite and nontronite when all analyzed components are included. However, XRD and EDS confirm that allophane is the most abundant weathering product, and there is no other crystalline phase present. Allophane is a common weathering product of younger (<10,000 ybp) volcanic ash deposits, and appears at early weathering stages relative to other crystalline phases (Dudas and Harward, 1975; Parfitt *et al*., 1983; Kawano *et al*., 1993). The K1 and K2 deposits are similarly composed mainly of volcanic glass and plagioclase and are young (4040 and 6400 ybp). An older rhyolitic pyroclastic deposit in Kagoshima Prefecture, Japan, which was deposited 22,000 y ago, contains mainly halloysite with smaller amounts of smectite and allophane (Kawano and Tomita, 1999). Thus, allophane in K1 and K2 may be present as a metastable phase, and would be transformed into halloysite or smectite depending on solution chemistry during subsequent weathering processes. On the other hand, neither deposit contains gibbsite, ferrihydrite or hematite despite the geochemical calculations of supersaturation. Gibbsite, a crystalline successor to amorphous $Al(OH)_3$, is a potential product of the weathering of pyroclastic glass. However, coexisting Si and Al ions tend to favor the formation of Al-Si minerals such as allophane over the formation of gibbsite (Wada *et al*.,

https://doi.org/10.1346/000986002761002865 Published online by Cambridge University Press

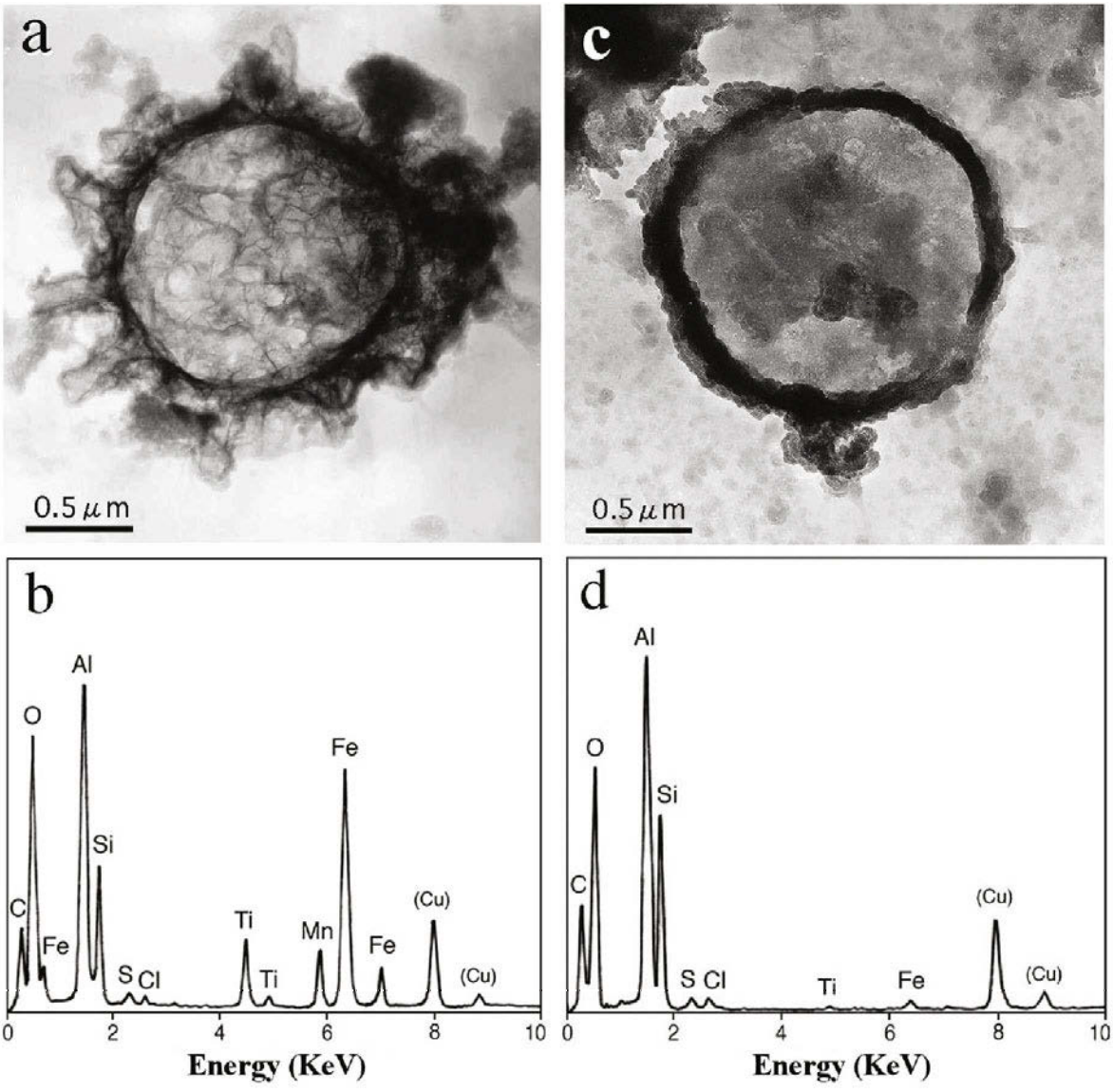

Figure 6. TEM micrographs and EDX spectra of: (a,b) microbiogenic poorly-ordered Al-Si-Fe minerals formed on the cell surface of a spherical bacterium; (c,d) granular precipitates of poorly-ordered Al-Si minerals associated with a spherical bacterium in the Koya pyroclastic flow deposit.

1979; Farmer *et al*., 1991). The formation of ferrihydrite and its recrystallization into hematite is similarly inhibited by Si ions (Schwertmann and Thalmann, 1976; Karim, 1984). The chemical environment of the K1 and K2 deposits may thus explain the absence of gibbsite, ferrihydrite and hematite.

Formation processes of microbiogenic minerals

The poorly-ordered Al-Si-Fe minerals on the bacterial cell surfaces are apparently formed by the initial binding of Al, Si or Fe to the cell walls, and subsequent growth under saturated conditions. This is inferred from TEM observations showing the presence of Al-Si-Fe minerals around the cell surfaces (Figures 6, 7). Bacterial cell surfaces act as favorable interfaces for the binding of metal ions and mineral growth (Schulte-Lam *et al*., 1996). The negatively charged sites exposed at the cell surfaces such as carboxyl (COO^-) and phosphoryl (PO_4^{3-}) groups serve as binding sites and they promote subsequent precipitation of various minerals on the cell surfaces (Beveridge, 1989). However, the formation of minerals in K1 and K2 cannot be explained by direct binding reactions of the predominant dissolved species with the bacterial cell surfaces because Si ions are predominantly present as neutral H_4SiO_4 and a very small fraction of of monovalent $H_3SiO_4^-$ anions at the pH of the porewaters (Iler, 1979). There are two possible mechanisms of Si binding and formation of silicate

https://doi.org/10.1346/000986002761002865 Published online by Cambridge University Press

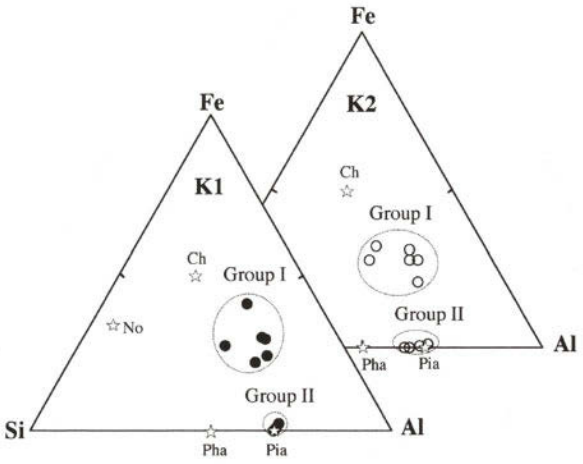

Figure 7. Chemical compositions of microbiogenic poorly-ordered Al-Si-Fe minerals (Group I) and granular precipitates of poorly-ordered Al-Si minerals (Group II) formed on the bacterial cell surfaces in the Kaimondake volcanic ash (closed circles) and the Koya pyroclastic flow (open circles) deposits plotted on the ternary diagrams of the Al-Si-Fe system. ☆: generalized compositions of some related clay minerals as follows; Ch: chamosite ($(Fe_5^{3+}Al)(Si_3Al)O_{10}(OH)_8$); No: nontronite ($Na_{0.33}Fe_2^{3+}(Si_{3.67}Al_{0.33})O_{10}(OH)_2$); Pha: proto-halloysite allophane (Al/Si = 1.0); Pia; proto-imogolite allophane (Al/Si = 2.0).

minerals: (1) binding of Si anions to positively charged sites such as amine groups in the cell wall matrix; and (2) binding of Si anions through bridging by metal ions bonded with negatively charged sites (Urrutia *et al.*, 1992). The former mechanism would be favored in acidic conditions because H^+ reduces the net negative charge of the cell surfaces, but there are not enough positive sites in the cell wall matrix to account for the large amounts of silica precipitation (Urrutia and Beveridge, 1994, 1995). Therefore, most silicate minerals developed on the bacterial surfaces have been presumed to be formed by the latter mechanism (Ferris *et al.*, 1987; Konhauser, 1998; Fortin and Beveridge, 1997).

For K1 and K2, there are two possible formation processes of Al-Si-Fe minerals on the bacterial surfaces. One is the binding of metal ions such as Al and Fe on the negative sites of bacterial cell walls and successive precipitation of monomeric Si ions. This process is fundamentally the same as that of mechanism 2, which occurs predominantly in solutions containing monomeric Si, Al and Fe. The other is the initial binding of hydroxy-aluminosilicate (HAS) complexed cations to the bacterial negative sites, and further deposition and polymerization of the complexed cations with the successive precipitation of Fe. The HAS ions have a similar structure to allophane, and are readily produced by interaction between hydrolyzed Al and Si ions (Wada *et al.*, 1979; Inoue and Huang, 1985; Wada *et al.*, 1988; Farmer *et al.*, 1991). The XRD analyses indicated that the weathering products of both deposits consist mainly of allophane with no gibbsite. This strongly suggests that Al and Si ions in the porewaters were present as HAS complexes, and precipitated metastably with Fe on the bacterial cell surfaces as poorly-ordered Al-Si-Fe minerals. This may be the predominant formation process for microbiogenic Al-Si-Fe minerals belonging to Group I (Figure 7), consistent with the results of Farmer *et al.* (1991).

Although the negatively charged bacterial cell surfaces promote precipitation of the initial solid phase, the transformation of this metastable phase into a more stable phase is essentially controlled by inherent thermodynamic properties of saturated minerals in the porewaters and by abiotic mineralization. Kawano and Tomita (2001a) reported a transformation process of poorly-ordered fibrous materials enriched in Al, Si and Fe to spherical halloysite during weathering of volcanic ash. They found that the transformation proceeds by the partial crystallization of a poorly-ordered matrix with a simultaneous decrease in Fe. A similar transformation has been observed on the surface of slightly weathered volcanic glass (Tazaki *et al.*, 1989; Kawano *et al.*, 1997). This is common in fully abiotic weathering systems, and the same reaction can be expected in microbiogenic minerals because biological processes do not influence the abiotic reaction. The microbiogenic Al-Si minerals belonging to Group II, therefore, may be a transitional phase from Group I to more stable crystalline phase such as allophane or halloysite. This transformation involves not only structural development but also a decrease in Fe content.

Impact of bacteria on mineral formation

Weathered rocks and sediments are the most common and widely distributed habitats of bacteria (Ehrlich, 1990; Barns and Nierzwicki-Bauer, 1997), but bacterial impacts on the formation of silicate minerals in such weathering environments are not clear. The results of this study show that the weathered pyroclastic deposits

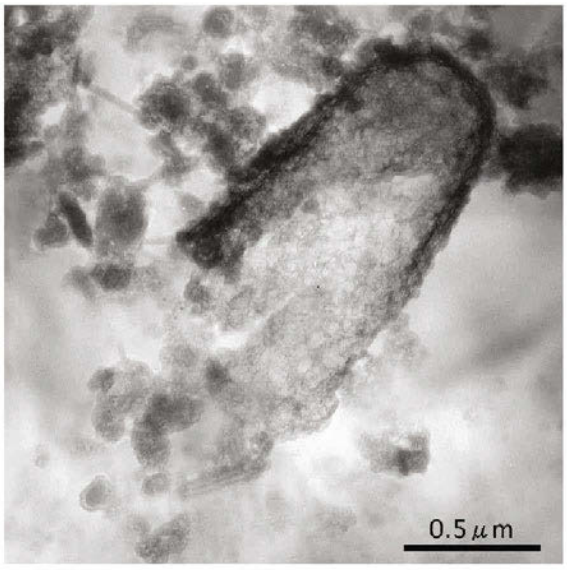

Figure 8. TEM micrograph showing dispersion processes of microbiogenic poorly-ordered Al-Si-Fe minerals into the surrounding environments by partial degradation of a bacterial cell.

we designated K1 and K2 contain 10^8–10^9 cells/g with microbiogenic Al-Si-Fe or Al-Si minerals on their cell surfaces. This observation suggests that bacteria play an important role in the formation of silicate minerals in weathering environments through the precipitation of minerals on their cell surfaces. Previous studies demonstrated that the interaction of negatively charged compounds on cell-wall surfaces with dissolved ions caused the accumulation of ions and the formation of minerals. Bacterial mineralization was confirmed by field observations (Beveridge, 1989; Ferris, 1993; Fortin and Beveridge, 1997; Konhauser and Urrutia, 1999; Kawano and Tomita, 2001b). Microbiogenic minerals are usually amorphous to poorly-ordered with variable chemical compositions, but over time they transform into crystalline phases having a specific chemical composition (Konhauser, 1998). In weathering environments on the terrestrial surface, bacterial precipitation of poorly-ordered metastable phases may occur continuously if the porewaters remain saturated with respect to these phases, with the transformation into more crystalline mineral phases proceeding thermodynamically, depending on solution chemistry. Bacterial mineralization must have persisted over geological time, with the production of significant amounts of microbiogenic minerals in weathered deposits. The TEM analysis showed that initial metastable phases of such microbiogenic minerals formed on the bacterial cell surfaces were distinct from co-existing abiotic products. However, the microbiogenic minerals were indistinguishable from the abiotic products when the cells decomposed after death. Although the lifetime of an individual bacterial cell in weathering environments is not well known, the decomposition of the cell after death would disperse the microbiogenic minerals precipitated on the cell surfaces and assimilate with the abiogenic weathering products present in the extracellular environment, as shown in Figure 8. This strongly suggests that some of the weathering products unassociated with bacteria, such as allophane in this study, may have been originally produced by bacteria or transformed from the poorly-ordered microbiogenic minerals. Similar bacterial mineralization may have occurred continuously over the terrestrial surface and over geological time.

ACKNOWLEDGMENTS

The authors thank Dr J.P. McKinley and Dr D.C. Bain for their useful comments and suggestions which helped to improve this manuscript. The transmission electron microscopy was performed in the Laboratory for High Voltage Electron Microscope at Kagoshima University. The scanning electron microscopy was conducted at the Department of Chemistry and Bioscience also at Kagoshima University. This study was supported financially by the Japanese Ministry of Education, Science, Sport and Culture (No. 80224814).

REFERENCES

Barns, S.M. and Nierzwicki-Bauer, S.A. (1997) Microbial diversity in ocean, surface and subsurface environments. Pp. 35–79 in: *Geomicrobiology: Interactions between Microbes and Minerals* (J.F. Banfield and K.H. Nealson, editor). Reviews in Mineralogy, **35**. Mineralogical Society of America, Washington, D.C.

Beveridge, T.J. (1989) Role of cellular design in bacterial metal accumulation and mineralization. *Annual Review of Microbiology*, **43**, 147–171.

Beveridge, T.J. and Fyfe, W.S. (1985) Metal fixation by bacterial cell walls. *Canadian Journal of Earth Science*, **22**, 1893–1898.

Bigham, J.M., Schwertmann, U., Carlson, L. and Murad, E. (1990) A poorly crystallized oxyhydroxysulfate of iron formed by bacterial oxidation of Fe(II) in acid mine waters. *Geochimica et Cosmochimica Acta*, **54**, 2743–2758.

Dudas, M.J. and Harward, M.E. (1975) Weathering and authigenic halloysite in soil developed in Mazama ash. *Soil Science Society of America Proceedings*, **39**, 561–566.

Ehrlich, H.L. (1990) *Geomicrobiology: Second Edition, Revised and Expanded*. Marcel Dekker, New York, 646 pp.

Farmer, V.C., Fraser, A.R. and Tait, J.M. (1979) Characterization of the chemical structures of natural and synthetic aluminosilicate gels and sols by infrared spectroscopy. *Geochimica et Cosmochimica Acta*, **43**, 1417–1420.

Farmer, V.C., Krishnamurti, G.S.R. and Huang, P.M. (1991) Synthetic allophane and layer-silicate formation in SiO-Al_2O_3-FeO-Fe_2O_3-MgO-H_2O systems at 23°C and 89°C in a calcareous environment. *Clays and Clay Minerals*, **39**, 561–570.

Fein, J.B., Daughney, C.J., Yee, N. and Davis, T. (1997) A chemical equilibrium model for metal adsorption onto bacterial surfaces. *Geochimica et Cosmochimica Acta*, **61**, 3319–3328.

Ferris, F.G. (1993) Microbial biomineralization in natural environments. *Earth Science*, **47**, 233–250.

Ferris, F.G., Beveridge, T.J. and Fyfe, W.S. (1986) Iron-silica crystallite nucleation by bacteria in a geothermal sediment. *Nature*, **320**, 609–611.

Ferris, F.G., Fyfe, W.S. and Beveridge, T.J. (1987) Bacteria as nucleation sites for authigenic minerals in a metal-contaminated lake sediment. *Chemical Geology*, **63**, 225–232.

Ferris, F.G., Tazaki, K. and Fyfe, W.S. (1989) Iron oxides in acid mine drainage environments and their association with bacteria. *Chemical Geology*, **74**, 321–330.

Fitzpatrick, R.W., Naidu, R. and Self, P.G. (1992) Iron deposits and microorganisms in saline sulfidic soils with altered soil water regimes in south Australia. Pp. 263–286 in: *Biomineralization: Processes of Iron and Manganese* (H.C.W. Skinner and R.W. Fitzpatrick, editors). Catena Verlag, Germany.

Fortin, D. and Beveridge, T.J. (1997) Role of the bacterium, *Thiobacillus*, in the formation of silicates in acidic mine tailings. *Chemical Geology*, **141**, 235–250.

Fortin, D., Ferris, F.G. and Scott, S.D. (1998) Formation of Fe-silicate and Fe-oxides on bacterial surfaces in samples collected near hydrothermal vents on the Southern Explorer Ridge in the northeast Pacific Ocean. *American Mineralogist*, **83**, 1399–1408.

Fouke, B.W., Farmer, J.D., Des Marais, D.J., Pratt, L., Sturchio, N.C., Burns, P.C. and Discipulo, M.K. (2000) Depositional facies and aqueous-solid geochemistry of travertine-depositing hot spring (Angel Terrace, Mammoth Hot Spring, Yellowstone National Park, USA). *Journal of Sedimentary Research*, **70**, 565–585.

Hannington, M.D. and Jonasson, I.R. (1992) Fe and Mn oxides at seafloor hydrothermal vents. Pp. 351–370 in: *Biomineralization: Processes of Iron and Manganese* (H.C.W. Skinner and R.W. Fitzpatrick, editors). Catena Verlag, Germany.

Hinman, N.W. and Lindstrom, R.F. (1996) Seasonal changes in silica deposition in hot spring systems. *Chemical Geology*, **132**, 237–246.

Iler, R.K. (1979) *The Chemistry of Silica*. John Wiley & Sons, New York, 866 pp.

Inoue, K. and Huang, PM. (1985) Influence of citric acid on the formation of short-range ordered aluminosilicates. *Clays and Clay Minerals*, **33**, 312–322.

Ishikawa, H., Arimura, K., Oki, K. and Maruno, K. (1979) ^{14}C ages of the Ata pyroclastic flow and the Kaimon volcanic ash bed in the Kagoshima Prefecture. *Journal of Geological Society of Japan*, **85**, 695–697 (in Japanese).

Jiang, W.-T., Peacor, D.R. and Buseck, P.R. (1994) Chlorite geothermometry? – contamination and apparent octahedral vacancies. *Clays and Clay Minerals*, **42**, 593–605.

Jones, B. and Renaut, R.W. (1996) Influence of thermophilic bacteria on calcite and silica precipitation in hot springs with water temperature above 90°C: Evidence from Kenya and New Zealand. *Canadian Journal of Earth Science*, **33**, 72–83.

Karim, Z (1984) Characteristics of ferrihydrites formed by oxidation of $FeCl_2$ solutions containing different amounts of silica. *Clays and Clay Minerals*, **32**, 181–184.

Kawano, M. and Tomita, K. (1999) Formation and evolution of weathering products in rhyolitic pyroclastic flow deposit, southern Kyushu, Japan. *Journal of Geological Society of Japan*, **105**, 699–710.

Kawano, M. and Tomita, K. (2001a) TEM-EDX study of weathered layers on the surface of volcanic glass, bytownite, and hypersthene in volcanic ash from Sakurajima volcano. *American Mineralogist*, **86**, 284–292.

Kawano, M. and Tomita, K. (2001b) Microbial biomineralization in weathered volcanic ash deposit and formation of biogenic minerals by experimental incubation. *American Mineralogist*, **86**, 400–410.

Kawano, M., Tomita, K. and Kamino, Y. (1993) Formation of clay minerals during low temperature experimental alteration of obsidian. *Clays and Clay Minerals*, **41**, 431–441.

Kawano, M., Tomita, K. and Shinohara, Y. (1997) Analytical electron microscopic study of the noncrystalline products formed at early weathering stages of volcanic glass. *Clays and Clay Minerals*, **45**, 440–447.

Konhauser, K.O. (1998) Diversity of bacterial iron mineralization. *Earth Science Reviews*, **43**, 91–121.

Konhauser, K.O. and Urrutia, M.M. (1999) Bacterial clay authigenesis: a common biogeochemical process. *Chemical Geology*, **161**, 399–413.

Konhauser, K.O., Fisher, Q.J., Fyfe, W.S., Longstaffe, F.J. and Powell, M.A. (1998) Authigenic mineralization and detrital clay binding by freshwater biofilms: the Brahmani river, India. *Geomicrobiology*, **15**, 209–222.

Mehra, O.P. and Jackson, M.L. (1960) Iron oxide removal from soils and clays by a dithionite-citrate system buffered with sodium bicarbonate. Pp. 317–342 in: *Clays and Clay Minerals, Proceedings of the 7th National Conference* (A. Swineford, editor). Pergamon Press, New York.

Parfitt, R.L., Russell, M. and Orbell, G.E. (1983) Weathering sequence of soils from volcanic ash involving allophane and halloysite, New Zealand. *Geoderma*, **29**, 41–57.

Parkhurst, D.L. and Appelo, C.A.J. (1999) *User's guide to PHREEQC (Version 2) – A computer program for speciation, batch-reaction, one-dimensional transport, and inverse geochemical calculations. Water-Resources Investigations Report 99-4259*, US Geological Survey, Denver, Colorado, 312 pp.

Percival, H. (1995) Relative stabilities of elected clay minerals in soils based on a critical selection of solubility constants. Pp. 462–468 in: *Clays Controlling the Environment, Proceedings of the 10th International Clay Conference* (G.J. Churchmann, R.W. Fitzpatrick and R.A. Eggleton, editors). CSIRO publishing, Australia.

Schopf, J.W. (1983) *Earth's Earliest Biosphere, Its Origin and Evolution*. Princeton University Press, New Jersey, USA, 543 pp.

Schultze-Lam, S., Ferris, F.G., Konhauser, K.O. and Wiese, R.G. (1995) In situ silicification of an Icelandic hot spring microbial mat: implications for microfossil formation. *Canadian Journal of Earth Science*, **32**, 2021–2026.

Schultze-Lam, S., Fortin, D., Davis, B.S. and Beveridge, T.J. (1996) Mineralization of bacterial surfaces. *Chemical Geology*, **132**, 171–181.

Schwertmann, U. and Thalmann, H. (1976) The influence of [Fe(II)], [Si], and pH on the formation of lepidocrocite and ferrihydrite during oxidation of aqueous $FeCl_2$ solutions. *Clay Minerals*, **11**, 189–200.

Tazaki, K. (2000) Formation of banded iron-manganese structures by natural microbial communities. *Clays and Clay Minerals*, **48**, 511–520.

Tazaki, K., Fyfe, W.S. and van der Gaast, S.J. (1989) Growth of clay minerals in natural and synthetic glasses. *Clays and Clay Minerals*, **37**, 348–354.

Tazaki, K., Ishida, H. and Fyfe, W.S. (1995) Calcite deposition in a hot spring microbial mat from Iceland. Pp. 30–37 in: *Clays Controlling the Environment, Proceeding of the 10th International Clay Conference* (G.J. Churchmann, R.W. Fitzpatrick and R.A. Eggleton, editors). CSIRO publishing, Australia.

Ui, T. and Fukuyama, H. (1972) ^{14}C age of the Koya pyroclastic flow deposit and range of the volcanic activities of volcanoes at southern Kyushu. *Journal of Geological Society of Japan*, **78**, 631–632 (in Japanese).

Urrutia, M.M. and Beveridge, T.J. (1994) Formation of fine-grained metal and silicate precipitates on a bacterial surface (*Bacillus subtilis*). *Chemical Geology*, **116**, 261–280.

Urrutia, M.M. and Beveridge, T.J. (1995) Formation of short-range ordered aluminosilicates in the presence of a bacterial surface (*Bacillus subtilis*) and organic ligands. *Geoderma*,

65, 149–165.

Urrutia, M.M., Kemper, M., Doyle, R. and Beveridge, T.J. (1992) The membrance-induced proton motive force influences the metal binding ability of *Bacillus subtilis* cell walls. *Applied Environmental Microbiology*, **58**, 3837–3844.

Wada, K., Wilson, M., Kakuto, Y. and Wada, S.-I. (1988) Synthesis and characterization of a hollow spherical form of monolayer aluminosilicate. *Clays and Clay Minerals*, **36**, 11–18.

Wada, S.-I., Eto, A. and Wada, K. (1979) Synthetic allophane and imogolite. *Journal of Soil Science*, **30**, 347–355.

(*Received 18 January 2001; revised 27 June 2001; Ms. 514*)